

Hydrodynamics beyond Navier-Stokes: Exact solutions to the lattice Boltzmann hierarchy

S. Ansumali

*School of Chemical and Biomedical Engineering,
Nanyang Technological University, 639798 Singapore*

I. V. Karlin*

*Aerothermochemistry and Combustion Systems Lab,
ETH Zurich, 8092 Zurich, Switzerland*

S. Arcidiacono

Paul Scherrer Institute, Combustion Research, 5232 Villigen PSI, Switzerland

A. Abbas

*School of Chemical and Biomedical Engineering,
Nanyang Technological University, 639798 Singapore, Singapore*

N. I. Prasianakis

*Aerothermochemistry and Combustion Systems Lab,
ETH Zurich, CH-8092 Zurich, Switzerland*

Abstract

Exact solution to the hierarchy of nonlinear lattice Boltzmann (LB) kinetic equations in the stationary planar Couette flow is found at non-vanishing Knudsen numbers. A new method of solving LB kinetic equations which combines the method of moments with boundary conditions for populations enables to derive closed-form solutions for all higher-order moments. Convergence of results suggests that the LB hierarchy with larger velocity sets is the novel way to approximate kinetic theory.

PACS numbers: 47.11.-j, 05.70.Ln

* Corresponding author

Emerging field of fluid dynamics at a micrometer scale becomes increasingly important due to fundamental engineering issues of micro-electromechanical systems [1]. Recently, much attention was attracted by the use the lattice Boltzmann (LB) models for simulation of microflows by a number of groups [2, 3, 4, 5, 6, 7, 8]. By now, it is understood that lattice Boltzmann models form a well-defined hierarchy based on discrete velocity sets with velocities defined as zeroes of Hermite polynomials [9] or rational-number approximations thereof [10]. The LB hierarchy constitutes a novel approximation of the Boltzmann equation and has to be considered as an alternative to more standard approaches such as higher-order hydrodynamics (Burnett or super-Burnett) or Grad's moment systems (for a review see, e. g. [11]). One salient feature of the LB hierarchy, which is crucial to the present study and eventually to any realistic application, is that it is naturally equipped with relevant boundary conditions derived from Maxwell-Boltzmann's theory [2].

Agreement between the LB simulations and kinetic theory [2], hydrodynamics with slip boundary conditions [7], and molecular dynamics [8] was reported. However, most of these numerical works rely on simulation with finite accuracy while the crucial question whether or not the kinetic equations underpinning the LBM method are valid physical models of microflow remains unanswered. Therefore, it is not surprising to read comments claiming, for example, that the slip flow in the LBM is due to discretization errors rather than a physical effect, ([12] and references therein). Thus, validity of LBM cannot be addressed unless a comparison to representative exact solutions is performed. It is needless to say that exact solutions to nonlinear kinetic equations in realistic geometries are very rare.

In this Letter, we show that the LB hierarchy of kinetic models admits a much more accurate treatment. In particular, we find closed-form analytical solutions to nonlinear kinetic equations of the LB hierarchy in the stationary planar Couette flow. Not only the slip velocity, but also the shear stress and the normal stress difference are evaluated in a closed form. Comparison to the kinetic theory demonstrates convergence of approximations with the increase of the number of velocities. In the nonlinear domain, even the first member of the LB hierarchy predicts nontrivial normal stress which is confirmed with a more microscopic direct simulation Monte Carlo (DSMC) method [13]. The accurate results obtained herein strongly suggest that the LB hierarchy should be considered as a novel general tool of kinetic theory rather than a plain solver for hydrodynamics.

Kinetic equations studied in this paper are two-dimensional isothermal discrete velocity

models with the Bhatnagar-Gross-Krook (BGK) nonlinear collision integral (for a derivation of these models from the Boltzmann-BGK equation see, e. g., [9, 10]),

$$\partial_t f_i + c_{i\alpha} \partial_\alpha f_i = -\frac{1}{\tau} (f_i - f_i^{\text{eq}}), \quad (1)$$

where summation convention is applied, τ is the relaxation time, and the equilibrium distribution is

$$f_i^{\text{eq}}(\rho, j_x, j_y) = w_i \left(\rho + \frac{j_\alpha c_{i\alpha}}{c_s^2} + \frac{j_\alpha j_\beta}{2\rho c_s^4} (c_{i\alpha} c_{i\beta} - c_s^2 \delta_{\alpha\beta}) \right). \quad (2)$$

Here $c_s = \sqrt{(k_B T_0)/m}$ is the speed of sound, T_0 is the reference temperature.

The first member of the LB hierarchy is the so-called *D2Q9* model where the discrete velocities $c_{i\alpha}$, $i = 0, \dots, 8$, and the weights w_i are

$$\begin{aligned} c_x &= \sqrt{3}c_s \{0, 1, 0, -1, 0, +1, -1, -1, +1\} \\ c_y &= \sqrt{3}c_s \{0, 0, 1, 0, -1, +1, +1, -1, -1\} \\ w &= (1/36) \{16, 4, 4, 4, 4, 1, 1, 1, 1\}. \end{aligned} \quad (3)$$

The model (1) conserves locally the density $\rho = \sum_{i=0}^8 f_i$ and the momentum density $j_\alpha = \sum_{i=0}^8 c_{i\alpha} f_i$ but not the energy. In the hydrodynamic limit, it recovers the Navier-Stokes equations with the kinematic viscosity $\nu = \tau c_s^2$.

We consider the planar Couette flow, where a fluid is enclosed between two parallel plates separated by a distance L . The bottom plate at $y = -L/2$ moves with the velocity U_1 and top plate at $y = L/2$ moves with the velocity U_2 (see Fig. 1). Let us introduce the mean free path $l = \sqrt{3}\tau c_s$ and the Knudsen number $\text{Kn} = l/L$. The solution for the x -velocity of the *D2Q9* model derived below reads:

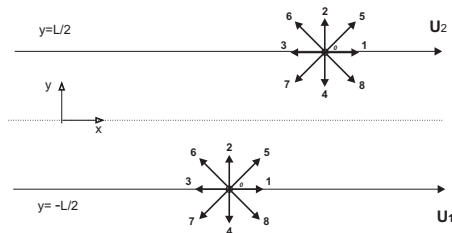


FIG. 1: Couette flow geometry. Discrete velocities of the *D2Q9* model at the bottom and the top plates are indicated to explain boundary conditions.

$$u_x = \frac{1}{\Theta_9} \left(\frac{y}{L} \right) \Delta U + U, \quad (4)$$

where

$$\Theta_9 = 1 + 2\text{Kn}, \quad (5)$$

and where $\Delta U = U_2 - U_1$ is the relative velocity of the plates, and $U = (U_1 + U_2)/2$ is the centerline velocity. Solution (4) is Galilean invariant: if a constant velocity C is added to both the plates, $U'_{1,2} = U_{1,2} + C$ then the velocity (4) transforms as $u'_x = u_x + C$. The slip velocity at the plates, $u_x(\pm L/2)$, features the expected behavior from a linear increase with Kn at small Kn to a plug flow at $\text{Kn} \rightarrow \infty$ where u_x becomes position-independent. Recent careful numerical study of the *D2Q9* model by Sofonea and Sekerka [7] revealed the same result (4) and (5).

The next member of the LB hierarchy is the model based on the roots of fourth-order Hermite polynomial $\{\pm a, \pm b\}$, where $a = \sqrt{3 - \sqrt{6}}$ and $b = \sqrt{3 + \sqrt{6}}$. In two dimensions, the discrete velocities are all possible tensor products of the two copies of the four-sets $\{\pm a, \pm b\}$. For this *D2Q16* model [9, 10], the solution for the velocity profile is found to be:

$$u_x = \frac{1}{Z_{16}} \sinh \left(\frac{y}{\text{Kn}L} \right) \Delta U + \frac{1}{\Theta_{16}} \left(\frac{y}{L} \right) \Delta U + U, \quad (6)$$

where

$$\Theta_{16} = 1 + 2\text{Kn} \left(\frac{2 \cosh \left(\frac{1}{2\text{Kn}} \right) + \mu \sinh \left(\frac{1}{2\text{Kn}} \right)}{\mu \cosh \left(\frac{1}{2\text{Kn}} \right) + 2\sqrt{3} \sinh \left(\frac{1}{2\text{Kn}} \right)} \right), \quad (7)$$

$$Z_{16} = \frac{\mu}{4\text{Kn}} \left((4\text{Kn} + \mu) \cosh \left(\frac{1}{2\text{Kn}} \right) + 2 \left(\mu\text{Kn} + \sqrt{3} \right) \sinh \left(\frac{1}{2\text{Kn}} \right) \right), \quad (8)$$

and $\mu = a + b \approx 3.076$. The difference between (4) and (6) is that the latter predicts the boundary Knudsen layer (first term in (6)) in a qualitative agreement with kinetic theory [14]. On the quantitative side, our analytical results can be immediately compared with the classical study of the linearized Boltzmann-BGK equation by Willis [15] (see Fig. 2, where also the results of the DSMC simulation are reported; note that data in Fig. 2 is parameterized with the Knudsen number according to a relation, $\text{Kn} = \sqrt{\frac{3}{2}}\alpha^{-1}$, where $\alpha = \frac{L}{\tau} \sqrt{\frac{m}{2k_B T_0}}$ is a parameter used in Table I of Ref. [15]). While the simplest *D2Q9* model predicts well a slip-flow solution, it fails in the transient regime ($\text{Kn} \gtrsim 0.1$), in agreement with numerical studies [2, 16]. However, already the *D2Q16* model considerably improves the situation. The strong pattern of convergence with increasing the number of velocities in the LB hierarchy is clearly there.

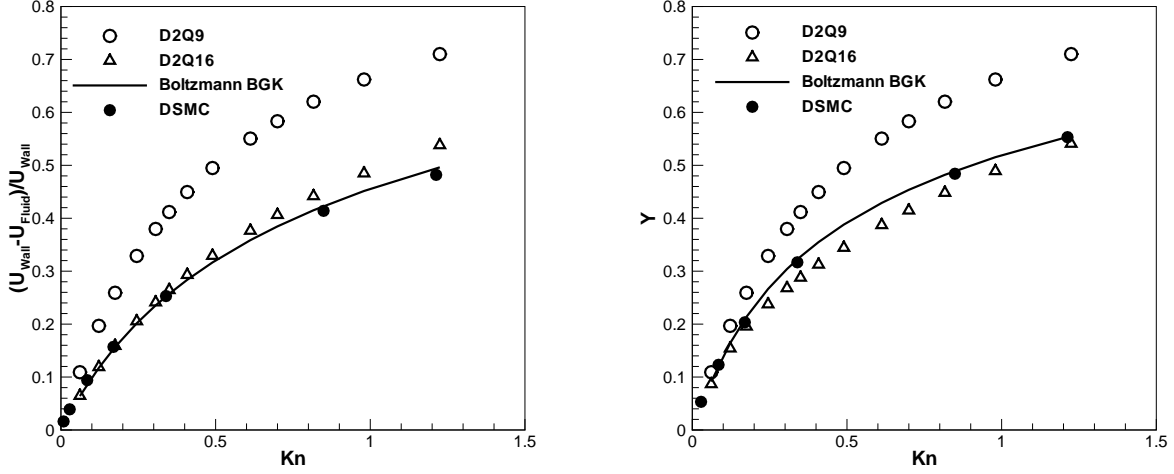


FIG. 2: Comparison of the LB hierarchy with the linearized Boltzmann-BGK model [15] and DSMC simulation. Left: Slip velocity at the wall as a function of Knudsen number. Right: Slope of the velocity profile at the centerline. Plotted is the deviation from the Navier-Stokes prediction, $Y = \Delta U^{-1}(du_x/dy)|_{y=0} - 1$.

We shall now proceed with major steps of derivation for the $D2Q9$ model. Firstly, we write the kinetic equation for nine populations (1) in a form of a moment system for nine moments which we choose as follows: Three locally conserved fields, ρ , j_x , j_y ; three independent components of the pressure tensor, $P_{\alpha\beta} = \sum_{i=0}^8 f_i c_{i\alpha} c_{i\beta}$, which we choose as the trace $P = P_{xx} + P_{yy}$, $N = P_{xx} - P_{yy}$ (normal stress difference), and P_{xy} ; two components of the energy flux, $q_\alpha = \sum_{i=0}^8 f_i c_{\alpha i} c_i^2$, and a scalar fourth-order moment, $\psi = R_{yyyy} + R_{xxxx} - 2R_{xxyy}$, where $R_{\alpha\beta\gamma\theta} = \sum_{i=0}^8 f_i c_{i\alpha} c_{i\beta} c_{i\gamma} c_{i\theta}$. The resulting moment system includes three balance equations for the locally conserved fields,

$$\begin{aligned}
\partial_t \rho + \partial_x j_x + \partial_y j_y &= 0, \\
\partial_t j_x + \frac{1}{2} \partial_x (P + N) + \partial_y P_{xy} &= 0, \\
\partial_t j_y + \partial_x P_{xy} + \frac{1}{2} \partial_y (P - N) &= 0,
\end{aligned} \tag{9}$$

three equations for the components of the pressure tensor,

$$\begin{aligned}\partial_t P_{xy} + \partial_x(q_y - 3c_s^2 j_y) + \partial_y(q_x - 3c_s^2 j_x) &= \frac{1}{\tau} \left(\frac{j_x j_y}{\rho} - P_{xy} \right), \\ \partial_t N + \partial_x(6c_s^2 j_x - q_x) + \partial_y(q_y - 6c_s^2 j_y) &= \frac{1}{\tau} \left(\frac{j_x^2}{\rho} - \frac{j_y^2}{\rho} - N \right), \\ \partial_t P + \partial_x q_x + \partial_y q_y &= \frac{1}{\tau} \left(2\rho c_s^2 + \frac{j^2}{\rho} - P \right),\end{aligned}\tag{10}$$

two equations for the components of the energy flux,

$$\begin{aligned}\partial_t q_x + \partial_x \left[3c_s^2 \left(P + \frac{1}{2}N \right) - \frac{1}{2}\psi \right] + 6c_s^2 \partial_y P_{xy} &= \frac{1}{\tau} (4c_s^2 j_x - q_x), \\ \partial_t q_y + 6c_s^2 \partial_x P_{xy} + \partial_y \left[3c_s^2 \left(P - \frac{1}{2}N \right) - \frac{1}{2}\psi \right] &= \frac{1}{\tau} (4c_s^2 j_y - q_y),\end{aligned}\tag{11}$$

and, finally, the equation for the fourth-order moment ψ ,

$$\partial_t \psi + 3c_s^2 \partial_x (6c_s^2 j_x - q_x) + 3c_s^2 \partial_y (6c_s^2 j_y - q_y) = \frac{1}{\tau} (4\rho c_s^4 + c_s^2 \frac{j^2}{\rho} - \psi).\tag{12}$$

Secondly, we find steady state solution to the moment system under two conditions: (i) Unidirectional flow: As the plates extend to infinity in the x direction, we can expect that the steady state solution will be independent of x , and (ii) Impermeable plates: The normal mass flux equals zero at the walls. For a unidirectional stationary flow, balance equations (9) read: $\partial_y j_y = 0$, $\partial_y P_{xy} = 0$, and $\partial_y(P - N) = 0$, whereupon, using condition (ii), we get $j_y = 0$, $P_{xy} = P_{xy}^{\text{neq}}$, $P = N + P_0$, where integration constants P_{xy}^{neq} and P_0 will be determined below (superscript ‘neq’ is added to emphasize that only the non-equilibrium part is nontrivial for P_{xy}). Furthermore, equation for the pressure tensor (10) reads

$$\partial_y(q_x - 3c_s^2 j_x) = -\frac{1}{\tau} P_{xy}^{\text{neq}},\tag{13}$$

$$\partial_y q_y = \frac{1}{\tau} \left(\frac{j_x^2}{\rho} - N \right),\tag{14}$$

$$\partial_y q_y = \frac{1}{\tau} \left(2\rho c_s^2 + \frac{j_x^2}{\rho} - N - P_0 \right),\tag{15}$$

From (14) and (15) it follows $P_0 = 2\rho c_s^2$. Thus, the stationary density is constant. Equation for energy flux (11) simplifies as:

$$q_x = 4c_s^2 j_x,\tag{16}$$

$$\partial_y \left[3c_s^2 \left(P - \frac{1}{2}N \right) - \frac{1}{2}\psi \right] = -\frac{1}{\tau} q_y.\tag{17}$$

Substituting (16) into (13), and integrating the resulting differential equation for j_x , we obtain the result for the nontrivial velocity component $u_x = j_x/\rho$,

$$u_x(y) = -\frac{\pi}{\tau c_s^2} (y + \tau V), \quad (18)$$

where V is constant of integration, and where we have introduced $\pi = P_{xy}^{\text{neq}}/\rho$. Thus, we find the solution for the velocity (up to two constants, π and V) *before* higher-order moments are addressed. We note in passing that it is precisely the relation (16) pertinent to the low-symmetry $D2Q9$ model (the energy flux is proportional to the momentum flux) which precludes the development of the boundary Knudsen layer. This constraint is removed in the more symmetric $D2Q16$ model and in any higher-order member of the LB hierarchy.

The stationary equation for fourth order moment ψ (12), together with (14), gives $\psi = 4c_s^2 \frac{j_x^2}{\rho} - 3c_s^2 N + 4\rho c_s^4$. Finally, from (17) and (14), we get

$$\partial_y q_y^{\text{neq}} = -\frac{N^{\text{neq}}}{\tau}, \quad \partial_y N^{\text{neq}} = -\frac{q_y^{\text{neq}}}{3\tau c_s^2} - \frac{\rho}{3} \partial_y (u_x^2). \quad (19)$$

The ordinary differential equations (19) can be integrated explicitly since the velocity $u_x(y)$ is available from (18). Denoting $\varphi(y) = \exp(y/\sqrt{3}\tau c_s)$, the result is

$$\begin{aligned} \sqrt{3} c_s N^{\text{neq}} + q_y^{\text{neq}} &= A\varphi(-y) - \frac{2\rho\pi^2}{\tau c_s^2} \left[y + \tau(V - \sqrt{3}c_s) (1 - \varphi(-y)) \right], \\ \sqrt{3} c_s N^{\text{neq}} - q_y^{\text{neq}} &= B\varphi(y) + \frac{2\rho\pi^2}{\tau c_s^2} \left[y + \tau(V + \sqrt{3}c_s) (1 - \varphi(y)) \right], \end{aligned} \quad (20)$$

where A and B are constants of integration. Thus, the solution to the stationary moment system depends on the four integration constants, π , V , A and B . In order to determine these, we need to specify boundary conditions at the moving plates. Note that this is precisely where the LB hierarchy differs from the method of moments. It is well known that for moment methods, such as Grad systems, it is not possible to provide self-consistent boundary conditions for the moments. In our case, this is possible because the boundary conditions for the LB equations are formulated in terms of populations rather than in terms of moments. Upon inverting the linear relation between the moments and the populations, and using the solution for the moments derived above, we obtain the stationary populations $f_i = f_i^{\text{eq}} + f_i^{\text{neq}}$, where the stationary equilibrium part is given by (2) with $j_y = 0$ and $j_x = \rho u_x$ (18), while the non-equilibrium part has the form,

$$f_i^{\text{neq}} = w_i \left(\frac{P_{xy}^{\text{neq}}}{c_s^4} c_{ix} c_{iy} + \frac{q_y^{\text{neq}}}{2c_s^6} (c_{iy} c_i^2 - 4c_s^2 c_{iy}) + \frac{N^{\text{neq}}}{2c_s^6} (c_{ix}^2 - c_s^2) c_{iy}^2 \right). \quad (21)$$

Thirdly and finally, we apply the classical diffuse boundary conditions [14], which were adapted to the present model in Ref. [2]. At the bottom plate ($y = -L/2$), diffuse boundary condition in the steady state is (see Fig. 1),

$$f_{2,5,6}|_{y=-L/2} = f_{2,5,6}^{\text{eq}}(\rho, \rho U_1, 0). \quad (22)$$

In other words, in the steady state, the diffuse boundary condition reduces to setting the corresponding populations at equilibrium (2) with the density ρ and velocity of the wall. Now, in order to find a relation between the two integration constants, V and π , we notice that the difference $[f_5^{\text{neq}} - f_6^{\text{neq}}]_{y=-L/2}$ can be evaluated in two ways. On one hand, $[f_i^{\text{neq}}]_{y=-L/2} = [f_i]_{y=-L/2} - [f_i^{\text{eq}}]_{y=-L/2}$, where the first contribution is due to (22), and the second is due to the stationary solution for the equilibrium (2) with the velocity (18), whereupon $[f_5^{\text{neq}} - f_6^{\text{neq}}]_{y=-L/2} = \frac{\sqrt{3}\rho}{18c_s}(U_1 + \frac{\pi}{\tau c_s^2}(-\frac{L}{2} + \tau V))$. On other hand, using (21), we find $[f_5^{\text{neq}} - f_6^{\text{neq}}]_{y=-L/2} = \frac{\rho\pi}{6c_s^2}$. Matching these expressions, we find a relation between integration constants π and V :

$$\pi = \frac{\sqrt{3}c_s U_1}{3 + \frac{\sqrt{3}}{\tau c_s}(\frac{L}{2} - \tau V)}. \quad (23)$$

Similarly, at the top plate ($y = L/2$, see Fig. 1), $f_{4,7,8}|_{y=L/2} = f_{4,7,8}^{\text{eq}}(\rho, \rho U_2, 0)$. Again, computing the difference $[f_7^{\text{neq}} - f_8^{\text{neq}}]_{y=L/2}$ in two ways as described above, we find:

$$\pi = -\frac{\sqrt{3}c_s U_2}{3 + \frac{\sqrt{3}}{\tau c_s}(\frac{L}{2} + \tau V)}. \quad (24)$$

Comparing (23) and (24), we find coefficients V and π , and, making use of (18), we arrive at the result for the velocity profile (4), while the non-equilibrium shear stress $P_{xy}^{\text{neq}} = \rho\pi$ reads

$$P_{xy}^{\text{neq}} = -\frac{\nu\rho}{\Theta_9} \left(\frac{\Delta U}{L} \right), \quad (25)$$

where Θ_9 is given by (5). Note that in the $D2Q16$ model the result for the shear stress is obtained by replacing Θ_9 with Θ_{16} (7). Results for the shear stress are compared with the data of Willis [15] and DSMC simulation in Fig. 3. In Tab. I, the limiting values of the effective shear viscosity, $\nu_{\text{eff}} = -P_{xy}^{\text{neq}}L(\Delta U\rho)^{-1}$, at the infinite Knudsen number for the $D2Q9$ and the $D2Q16$ LB models are compared with the Boltzmann-BGK result [15].

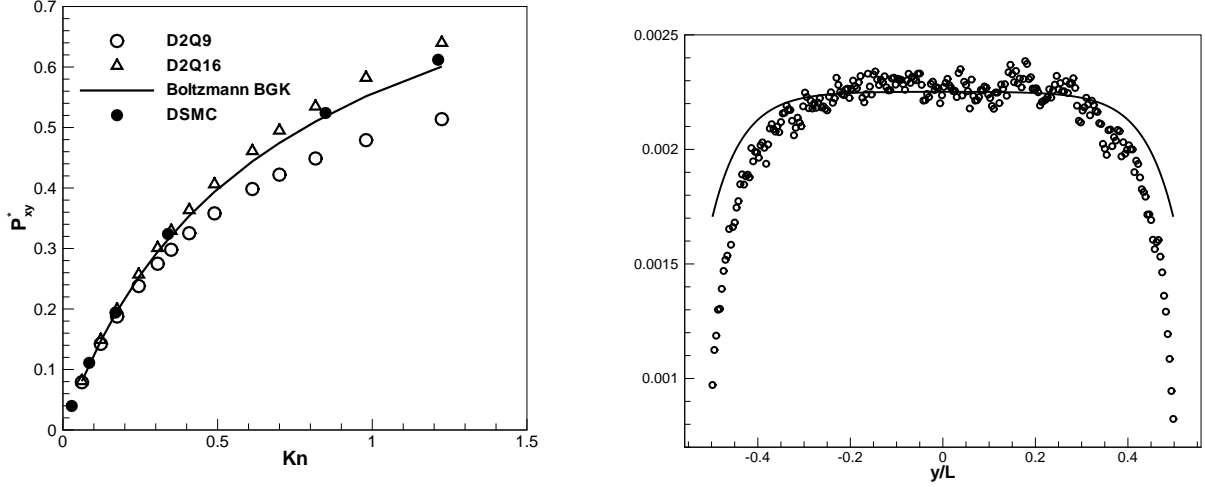


FIG. 3: Left: Shear stress at various Knudsen numbers. Labels are as in Fig. 2. Plotted is the reduced function $P_{xy}^* = P_{xy}/P_{xy}^\infty$ where P_{xy}^∞ is the shear stress at $\text{Kn} \rightarrow \infty$ of the Boltzmann-BGK model [15]. Right: Nonequilibrium normal stress difference at $\text{Kn} = 0.6$. Line: solution (26); Symbol: DSMC simulation.

$D2Q9$	0.723
$D2Q16$	1.113
BGK [15]	1

TABLE I: Effective shear viscosity ν_{eff} at $\text{Kn} \rightarrow \infty$, in units of $\sqrt{\frac{k_B T_0}{2\pi m}} L$ [15].

Same method is used in order to evaluate the two remaining integration constants A and B . Namely, we evaluate f_2^{neq} (bottom plate) and f_4^{neq} (top plate) in the two ways as described above. After some algebra, we find the results for the non-equilibrium normal stress difference and the transversal energy flux

$$N^{\text{neq}} = \rho \left(\frac{\Delta U}{L} \right)^2 \frac{\tau \nu}{(1 + 2\text{Kn})^2} \left[2 - e^{-\frac{1}{2\text{Kn}}} \cosh \left(\frac{y}{\text{Kn}L} \right) \right], \quad (26)$$

$$q_y^{\text{neq}} = -\rho \left(\frac{\Delta U}{L} \right)^2 \frac{\nu}{(1 + 2\text{Kn})^2} \left[2y - \text{Kn}L e^{-\frac{1}{2\text{Kn}}} \sinh \left(\frac{y}{\text{Kn}L} \right) \right] + 2UP_{xy}^{\text{neq}}. \quad (27)$$

Expressions for the velocity u_x (4), the shear stress P_{xy}^{neq} (25), the normal stress difference N^{neq} (26), and the energy flux q_y^{neq} (27), when substituted into $f_i = f_i^{\text{eq}} + f_i^{\text{neq}}$ (see (2) and (21)), furnish the exact solution of Couette flow for the nonlinear $D2Q9$ model. The same solution method is applicable to any member of the LB hierarchy although algebra becomes

more involved. Solution of the $D2Q16$ model leading to the result (6) will be presented in a detailed publication.

We have already mentioned that the solution for the velocity (4) is Galilean invariant. Same holds also for the higher-order moments. Indeed, the stress tensor is obviously Galilean invariant (that is, P_{xy}^{neq} (25) and N^{neq} (26) depend only on $U_2 - U_1$), and also the energy flux transforms correctly under $U'_{1,2} = U_{1,2} + C$: from the definition of the energy flux $q'_y = q_y + 2CP_{xy} + C^2j_y$, which is manifested in (27) ($j_y = 0$ in the present solution). The normal stress difference (26) is a positive-definite function which is consistent with kinetic theory of gases. Importantly, the nonvanishing of N^{neq} and q_y^{neq} is the direct implication of the nonlinearity of the kinetic equation (1) (manifested by the ΔU^2 dependence in (26) and (27)), and cannot be predicted on the basis of linearized kinetic theory [14, 15]. For that reason, the DSMC method [13] was used in order to validate the solution in the nonlinear domain. Parameters of the DSMC simulation correspond to the hard sphere model of Argon at normal conditions and diffuse scattering at the walls was implemented. The value of the velocity $U_1 = -U_2 = 0.5C_s$, where $C_s = \sqrt{5k_B T/3m}$ is the speed of sound of the three-dimensional ideal gas, was used to maintain a quasi-isothermal flow. The normal stress difference (26) is mapped onto DSMC data in Fig. 3 which qualitatively confirms the prediction.

Finally, in view of the concerns mentioned in the introduction, we validate the lattice Boltzmann method for the kinetic equation (1). The LB space-time discretization of (1) is standard, see, e. g. [17]. Simulation setup used corresponds to $U_1 = 0$, periodic boundary conditions were applied in the x -direction. Simulation were run till the steady state was reached, a grid convergence study was also performed. It is evident in Fig. 4 that the simulated relative slip accurately reproduces the exact solution (4). Same holds for all other moments. Thus, applications of the LBM to microflows are by no means an “artifact of numerics” [12]. Importance of physically relevant boundary conditions must be stressed. We have verified that if the standard “bounce-back” boundary condition of the LB method is used in the present problem, then the analytical result predicts vanishing slip velocity at all Knudsen numbers; thus, results of micro-flow simulations with the “bounce-back” boundary conditions or their derivatives are questionable indeed [18].

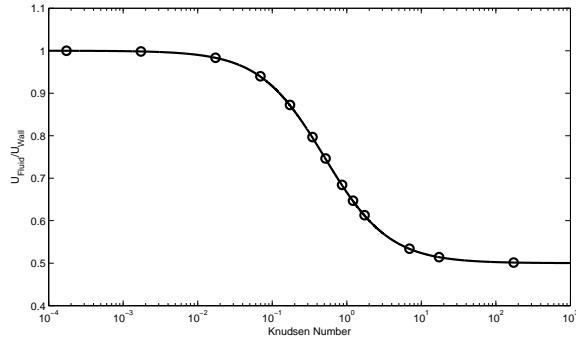


FIG. 4: Exact solution for the relative slip velocity (line) and the lattice Boltzmann simulation (symbol) as a function of Knudsen number.

To conclude, our analytical results suggest that the hierarchy of lattice Boltzmann models is the way to approximate the kinetic theory. Without a denial of a body of LB simulations, it must be appreciated that only the exact solutions answer unambiguously the question of the physical validity of the method. Our results reveal that applications to LB methods to microflows should be based on LB models with larger velocity sets if one seeks a quantitative prediction, especially in the transient regime. It would be quite interesting to extend the approach developed herein to obtain closed-form solutions in other cases of kinetic theory [14], and eventually also to three-dimensional cases. In that respect, we were able to extend the present analysis to the three-dimensional $D3Q27$ model, results will be reported elsewhere.

We acknowledge useful discussions of some of the results with G. Doolen, H.C. Öttinger, S. Succi and V. Yakhot. Support by BFE Project 100862 (I.V.K.), by the ETH Project 0-20235-05 (N.I.P), by CCEM-CH (I.V.K. and S.A.) and by NTU Office of Research (S.A.) is gratefully acknowledged.

-
- [1] A. Beskok and G. E. Karniadakis, *Microflows: Fundamentals and Simulation* (Springer, Berlin, 2001).
 - [2] S. Ansumali and I. V. Karlin, Phys. Rev. E **66**, 026311 (2002).
 - [3] S. Succi, Phys. Rev. Lett. **89**, 064502 (2002).
 - [4] B. Li and D. Kwok, Phys. Rev. Lett. **90**, 124502 (2003).
 - [5] X. D. Niu, C. Shu, and Y. Chew, Europhys. Lett. **67**, 600 (2004).

- [6] S. Ansumali and I. V. Karlin, Phys. Rev. Lett. **95**, 260605 (2005).
- [7] V. Sofonea and R. Sekerka, J. Comput. Phys. **207**, 639 (2005).
- [8] J. Horbach and S. Succi, Phys. Rev. Lett. **96**, 224503 (2006).
- [9] S. Ansumali, I. V. Karlin, and H. C. Öttinger, Europhys. Lett. **63**, 798 (2003).
- [10] S. S. Chikatamarla and I. V. Karlin, Phys. Rev. Lett. **97**, 190601 (2006).
- [11] A. N. Gorban and I. V. Karlin, *Invariant Manifolds for Physical and Chemical Kinetics* (Springer, Berlin, 2005).
- [12] L.-S. Luo, Phys. Rev. Lett. **92**, 139401 (2004).
- [13] G. A. Bird, *Molecular Gas Dynamics and the Direct Simulation of Gas Flows* (Clarendon Press, Oxford, 1994).
- [14] C. Cercignani, *Theory and Application of the Boltzmann Equation* (Scottish Academic Press, Edinburgh, 1975).
- [15] D. R. Willis, Phys. Fluids **5**, 127 (1962).
- [16] Z. Guo, T. S. Zhao, and Y. Shi, J. Appl. Phys. **99**, 074903 (2006).
- [17] X. He, S. Chen, and G. D. Doolen, J. Comput. Phys. **146**, 282 (1998).
- [18] C. Shen, D. B. Tian, C. Xie, and J. Fan, Microscale Thermophys. Eng. **8**, 423 (2004).